Response to reviewer's comments:

We want to thank the reviewer for the detailed and critical review. The valuable comments have improved the quality of the paper by making the objective, the probabilistic simulation approach, and the connectivity of the two parts much clearer. Furthermore, the comments helped us to re-write the paper in order to provide more precise information on the methods used and the underlying assumptions.

In the following, you can find our answers to the comments. A revised version of the manuscript is prepared and the corresponding paragraphs are marked in the manuscript. Pages and lines used in the answers refer to the new version.

General response concerning the overall simulation approach and the main objectives:

First of all, we want to give a general response concerning the overall (probabilistic) simulation approach in section 3 and the main objective of this work, as both is obviously not clear enough. These explanations are now included in the paper section 3.1 to make it clearer to the reader.

The main objective of this work is to provide a data basis for scattering environmental conditions and to give practical recommendations. Both is intended to make future simulations more realistic and reliable. We do not want to present a precise methodology to calculate ULS and FLS loads for turbine design or optimisation.

Many simulation approaches in academia focus on power production load cases (e.g. [1-3]), as other load cases are, firstly, frequently less relevant (e.g. for the considered jacket [4]), secondly, are very controller and design dependent, and thirdly, need special treatment (e.g. simulation lengths and initial transient times can be completely different). Therefore, this work intends to give guidance on simulation lengths and initial transient times for future work in academia focussing on power production, if scattering environmental conditions are applied.

This main objective leads to three implications:
   a) There is no need of "perfect" FLS/ULS calculation, as the objective is not the computation of the lifetime of the turbine or a new design (we do not perform turbine design according to the standards), but the investigation of simulation constraints.
   b) Consequently, there is no need to simulate all load cases. Start up, shut down and other "special" load cases need special treatment anyway (simulation constraints will be different compared to power production load cases), and therefore, are not investigated here.
   c) The approach of using scattering environmental conditions leads to "real-life" simulation and not a "load case based" simulation. This means that the simulation shall represent the real lifetime of the turbine (without fault, start-up, etc.). Hence, the simulations (e.g. 10000 simulations) cover a period of power production and idling, leading to 2.3 months of turbine lifetime (for 10000 simulations). As environmental conditions scatter, effects like high turbulences, extreme wind shear, high waves, small wave periods, and others are covered and do not have to be considered separately. Load cases are not simulated explicitly, but are cover implicitly by conducting probabilistic simulations.
   That is why for FLS, the two approaches do not significantly differ. The "real-life" approach covers DLC 1.2 and 6.4. For ULS, the "real-life" approach covers all power production cases (DLC 1.1-1.6) and DLC 6.1 by applying scattering environmental conditions. As the "real-life" approach cannot simulate 20 years of turbine lifetime (or even a return period of 50 years), a load extrapolation, as required for DLC 1.1, is needed in order to calculate a "perfect" ULS design. However, this extrapolation is not needed here, as it does not influence the investigated simulation constraints.

Whether this probabilistic "real-life" approach represents the turbine life correctly is not investigated here, as this is not of primary significance (see a)). In any case, simulation constraints for power production load cases can be analysed with this procedure, as all these load cases are covered.

1.) *A number of environmental variables including air and water density, currents etc. are captured in section 2 for the 3 offshore sites. However section 3 on the analysis of load simulations essentially investigates simulation length time and initial transience. As it stands, section 2 and section 3 are not well connected and there needs to be a clear explanation made as to how the varying environmental conditions modeled in section 2 are used in the load simulations. Without this connectivity, the paper cannot be published.*

You are right, that, as it stands, it was not clear enough that scattering environmental conditions, being derived in section 2, are applied for all simulations in section 3. This should now be much clearer. Firstly, in section 3.2, the application of statistically scattering values in all simulations is now mentioned. Secondly, section 3 was complemented by a detailed explanation of the overall simulation approach according to the "general response" above (section 3.1). This makes the use of scattering environmental conditions in the "real-life" approach clear, and therefore, connects the two sections.

2.) *Similarly to point 1 above, about 2 pages of the manuscript are devoted to analysis of ocean currents, but ocean currents are not used in fatigue load simulations as per the IEC 61400-3 and may have only limited influence on extreme loads. So this analysis on pg. 6-7 can be deleted, unless shown in section 3 to be relevant.*

It is correct that the influence of ocean currents is limited and not used for the FLS simulations according to IEC 61400-3. However, due to several reasons, the authors regard the inclusion of statistical distribution for ocean currents as beneficial. Firstly, according to IEC 61400-3, ocean currents have to be included in the ULS calculation. Therefore, for these load cases a statistical, more realistic representation of ocean currents might be valuable. Secondly, although the influence of currents on ULS loads is limited, it is not neglectable [5]. Thirdly, the current data basis is intendent to be slightly more general and hopefully relevant for some other applications as well. Hence, even if ocean currents would not influence ULS loads (which is not the case), the inclusion of ocean currents in the data basis might be useful for application concentrating on hydrodynamic effects.
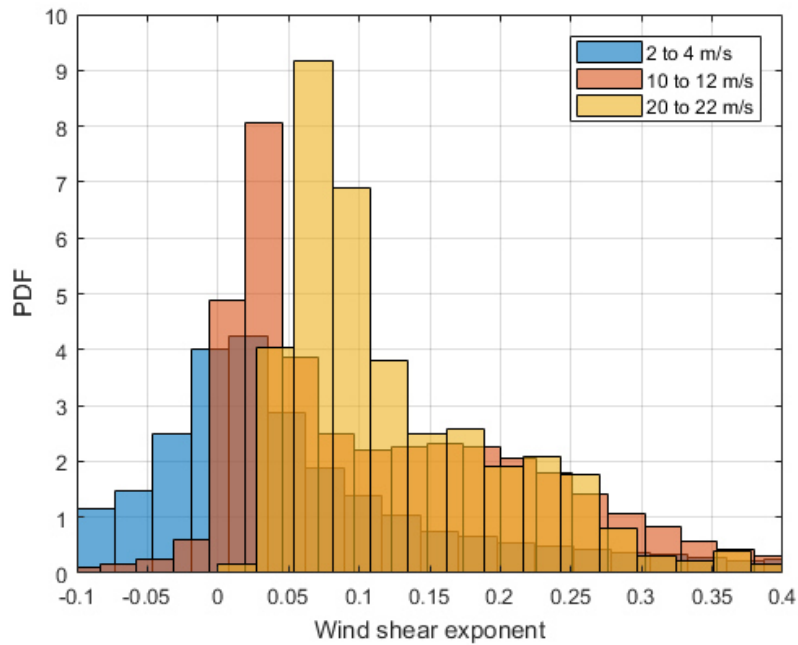Therefore, in section 3, it does not have to be shown that ocean currents are relevant for FLS or ULS loads. Sensitivity analyses for all parameters are out of the scope of this paper, but could use the provided statistical distributions [5].

3.) *Figure 7 on the probability of the wind shear exponent is not clear and it is not evident why the probability of a higher wind shear exponent is greater for higher mean wind speed bins. It would be more appropriate, if the shear exponent probability is plotted for different atmospheric stability classes.*
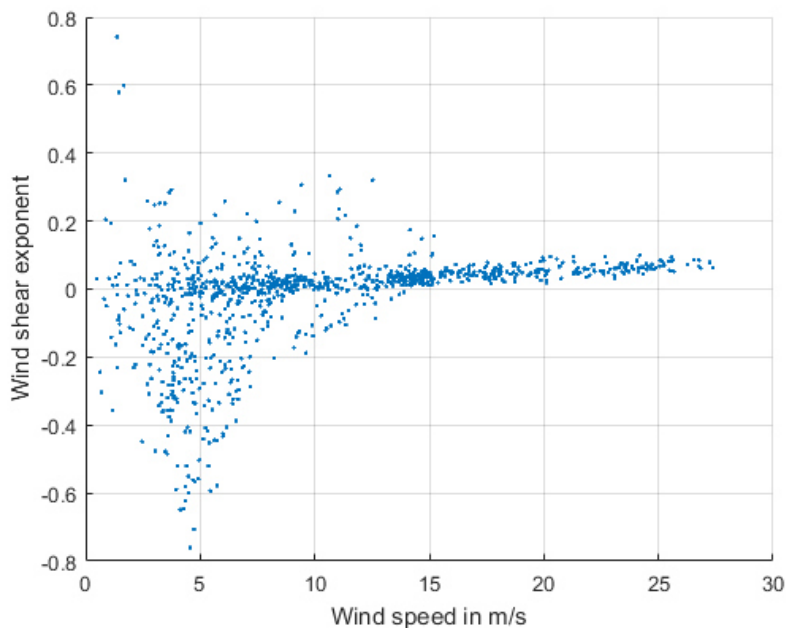
It is right that a correlation between the shear exponent and the atmospheric stability is probably more common. However, there is also a correlation between atmospheric stability and wind speed with higher stabilities for higher wind speeds [6]. Therefore, it is also possible to correlate wind speed and wind shear.
Additionally, the distributions given in Fig. 7 are based on real data. If you consider the following figures, you can firstly see the real data histograms for three different wind speeds. Secondly, there is a correlation plot for the wind speed and the wind shear exponent. Therefore, it is evident that, for the considered sites, higher wind shear exponents occur at higher wind speeds. This feature has also been detected in [6, 7] for example.

A phenomenological investigation of the reasons for this feature is out of the scope of this work, as this work is data based.

Real data histograms of wind shear exponents depending on the wind speed (FINO2 data)

Correlation plot: Wind speed versus for wind shear exponents with increasing mean wind shear (For reasons of clarity, only one week of FINO2 data is used. The use of all data features the same correlation, but due to more than 100 000 data points the plot gets unclear)

4.) In Section 3.1, it is not at all clear how the fatigue damage in welded joints of the monopile and jacket are computed. How are the stress concentration factors at the welded joint computed? How is the circumferential variation of the wind direction over a year modeled especially for the simulation on jackets? What type of jacket joints are considered - K joint, Y joint etc? Without these details, the analysis of fatigue on sub structures is inadequate and incomplete.

The explanations in section 3.2 (formerly 3.1) are definitively too brief to be clear. Therefore, the paragraph on fatigue calculation using current standards is improved by giving more details.

First, the procedure is clarified: Due to the statistical variation of the environmental conditions that is applied, the conducted simulations represent a typical part of the turbines lifetime (without failure and start-up cases etc.). For example, 10000 simulations represent about 2.3 months of realistic turbine lifetime. Directional variations of the wind are already included by just applying the scattering environmental conditions. Hence, summing up the damages of all ten-minute simulations gives a realistic estimate of the damage occurring during this time (e.g. 2.3 months). Surely, the damages in each joint and even each connection of the joint are different, and the highest damages do not occur in the same joint connection for each simulation (for example due to the variation in the wind direction). Therefore, for the connections of all joints (K-joints, Y-joints, butt-welds, …) the summation over all simulations is done separately, leading to overall damages (2.3 month damages) for each joint connection. Now, the highest accumulated damage value of all joint connections is used to be the jacket damage as it is the most critical one.

Second, the damage calculation for each simulation is clarified: For the jacket, DNV-RP-C203 is applied. For each connection to a joint, eight spots around the circumference of the intersection are calculated according to section 3.3.2 (of DNV-RP-C203). The needed SCFs are computed according to Appendix B for different joint geometries. For the monopile, Eurocode 3, part 1-9 is used. Guidance on stress producing effects of details and welds is given in Table 8.1 to 8.10. For the monopile, a detail of 71 MPa for transverse butt welds (longitudinal welds have higher details, and therefore, are less critical) is used. Furthermore, an additional reduction due to the size effect (t>25mm, c.f. Table 8.3) is applied.

5.) What load case is analyzed in section 3.2 to compute fatigue damage? Is it only DLC 1.2? What about DLC 6.4, DLC 7.2, 4.1 etc?

As stated in the general response, for fatigue, the probabilistic approach covers implicitly DLC 1.2 and 6.4. Other, "special" load cases are not analysed due to the three already mentioned reasons: Limited relevance (e.g. for the jacket [4]), controller and design dependence, special treatment due to different simulations constraints (e.g. initial transients are relevant for physical turbine start-ups (DLC3)), and no "perfect" fatigue calculation needed.

6.) *In Figure 10 and 11, is it the fatigue damage that is plotted or the damage equivalent load?*

Figure 10 and 11 show the mean fatigue damage that is normalised with the six-hour values as stated on p.14. The procedure how these values are calculated should now be explained much clearer (additional section on the overall simulation setup (section 3.1), and paragraphs on the fatigue model (p.12-13), and on the statistical calculation procedure (p.13-14)) .

7.) It is not clear how the half-cycles are merged in Fig. 11 and why the variation in fatigue damage suddenly disappears above 1-hour of simulation.

The procedure of merging several times series to eliminate the effects of half cycles is explained on p.14-15 and is now further elaborated. In Fig. 11 "not merged" case, it can be seen that, for simulation lengths below about two hours, the normalised mean fatigue damage is lower than for the converged case (six hours simulation length). This is due to unclosed half cycles in each time series. For long simulations, the effect of half cycles can be neglected, as the number of unclosed cycles is small compared to the number

of closed cycles. Therefore, it is possible to eliminate this effect in short simulations (e.g. ten-minute simulations) by merging each short simulations several times with itself. This means: Each ten-minute time series is duplicated and then appended several times to itself until a six-hour time series is formed consisting of 36 identical ten-minute time series. For this generic and repeating six-hour time series, the ratio of unclosed cycles to closed cycles is small enough in order to eliminate the effect of half cycles.

The reason for disappearing variations in fatigue damages for longer simulations is twofold. Firstly, in Fig. 11, there was a numerical problem. Due to too few significant numbers used, small variations were rounded to zero. This is now removed and Fig. 11 is revised. However, secondly, the uncertainty actually reduces for longer simulations. This is due to the fact that the overall length (simulation length multiplied by number of simulations) increases. This effect of not keeping the overall length constant is - in another context - discussed in section 3.3 for ULS loads (Fig. 12 and 13).

8.) *Explain what load cases are simulated for ULS loads in Fig 12 and 13 and what is the annual return probability of the ULS loads computed?*

Similar to remark 5), the simulated load cases are explained in the general response and are now included in section 3.1. Load cases according to the standards are not simulated separately, but a "real-life" approach is applied. "Special" load cases (start-up, etc.) are not included. For power production and idling, the "real-life" approach covers DLC 1.1, DLCs 1.3 to 1.6, and DLC 6.1 as environmental conditions are varied. Consequently, the conducted simulations do not represent classical extreme event simulations with specific return periods, but act as a realistic lifetime period (e.g. 2.3 months for 10000 simulations) that can be extrapolated to 20 or 50 years, by applying extrapolation methods like those for DLC1.1. This extrapolation is not done here, as the focus of this work is not on ULS values, but on simulations constraints for ULS simulations that are not influenced by the extrapolation.

9.) *The start-up time for load simulations depends on the time constants of the aeroelastic models, the frequencies of the turbine and the numerical solver used, besides the damping that is referred to in the paper. So table 3 is highly aeroelastic code and turbine model dependent and cannot be used as a general recommendation.*

So far, it was not explicitly stated that Table 3 cannot be used as a general recommendation. This was now revised, and the additional limitations you mentioned are included. However, these values are still relevant due to two reasons: Firstly, for similar applications (FASTv8, NREL 5MW turbine, etc.) that are not rare in academia (e.g. [1, 2, 8, 9]) the values might be used. And secondly, even more important, these results can sensitise other researches to the problem of initial transients especially in case of fatigue. For fatigue, times of initial transients might be higher than expected or applied in literature, and a pure glance on time series is not sufficient, as less damped cycles with small amplitudes cannot directly be seen/identified.

Overall the paper is presenting results without appropriate explanation of the load cases used, the limitations of the analysis, the justification of the methods used and the underlying assumptions. It needs to be re-written to provide clear and relevant justification of the results and methods.

The paper was rewritten in order to provide a much clearer presentation of the methods used and of their limitation. Especially, section 3 was enhanced by an extensive explanation of the overall simulation approach (section 3.1). This extension of the paper clarifies the load cases covered without directly simulating load cases according to the standards, but applying a probabilistic approach. Furthermore, it makes clear the limitations concerning the non-covered load cases and the FLS and ULS calculations that are not "perfect" and not suitable for a design procedure. However, it justifies why, for the present objective of giving recommendations for simulation constraints, this approach is sufficient.

For other aspects (e.g. wind shear, ocean currents), justifications for the utilized methods are given in this response to the comments.

The limitation concerning the general validity of times of initial transients are stated more precisely, but the remaining benefit is highlighted as well.

[1] Morató, A., Sriramula, S., Krishnan, N., & Nichols, J. (2017). Ultimate loads and response analysis of a monopile supported offshore wind turbine using fully coupled simulation. *Renewable Energy*, *101*, 126-143.

[2] Zwick, D., & Muskulus, M. (2015). The simulation error caused by input loading variability in offshore wind turbine structural analysis. *Wind energy*, *18*(8), 1421-1432.

[3] Haid, L., Stewart, G., Jonkman, J., Robertson, A., Lackner, M., & Matha, D. (2013, June). Simulation-length requirements in the loads analysis of offshore floating wind turbines. In *ASME 2013 32nd International Conference on Ocean, Offshore and Arctic Engineering* (pp. V008T09A091-V008T09A091). American Society of Mechanical Engineers.

[4] N.K. Vermula, Deliverable D4.2.5-WP4.2: Offshore Foundations and Support Structures, UpWind Project, 2010.

[5] Hübler, C., Müller, F., Gebhardt, C. G., & Rolfes, R. (2017). Global Sensitivity Analysis of Offshore Wind Turbine Substructures. In *Proceedings of the 15th International Probabilistic Workshop*, accepted for publication.

 [6] Holtslag, M. C., Bierbooms, W. A. A. M., & Van Bussel, G. J. W. (2014). Estimating atmospheric stability from observations and correcting wind shear models accordingly. In *Journal of Physics: Conference Series* (Vol. 555, No. 1, p. 012052). IOP Publishing.

[7] Ernst, B., & Seume, J. R. (2012). Investigation of site-specific wind field parameters and their effect on loads of offshore wind turbines. *Energies*, *5*(10), 3835-3855.

[8] Ziegler, L., & Muskulus, M. (2016, September). Fatigue reassessment for lifetime extension of offshore wind monopile substructures. In *Journal of Physics: Conference Series* (Vol. 753, No. 9, p. 092010). IOP Publishing.

[9] Amirinia, G., & Jung, S. (2017). Buffeting response analysis of offshore wind turbines subjected to hurricanes. *Ocean Engineering*, *141*, 1-11.

Development of a comprehensive data basis of scattering environmental conditions and simulation constraints for offshore wind turbines

Clemens Hübler[1], Cristian Guillermo Gebhardt[1], and Raimund Rolfes[1]

[1]Institute of Structural Analysis, Leibniz Universität Hannover, Appelstr. 9a, D-30167 Hannover, Germany

Correspondence to: Clemens Hübler (c.huebler@isd.uni-hannover.de)

Abstract. For the design and optimisation of offshore wind turbines, the knowledge of realistic environmental conditions and utilisation of well-founded simulation constraints is very important, as both influence the structural behaviour and power output in numerical simulations. However, real high-quality data, especially for research purposes, is scarcely available. This is why, in this work, a comprehensive data basis of thirteen environmental conditions at wind turbine locations in the North and Baltic Sea is derived using data of the FINO research platforms. For simulation constraints, like the simulation length and the time of initial simulation transients, well-founded recommendations in literature are also rare. Nevertheless, it is known that the choice of simulation lengths and times of initial transients fundamentally affects the quality and computing time of simulations. For this reason, studies of convergence for both parameters are conducted to determine adequate values depending on the type of substructure, the wind speed and the considered loading (fatigue or ultimate). As the main purpose of both the data basis and the simulation constraints is to compromise realistic data for probabilistic design approaches and to serve as a guidance for further studies in order to enable more realistic and accurate simulations, all results are freely available and easy to apply.

1 Introduction

Although the share of offshore wind energy in overall energy production has been steadily growing over the last years, the cost of offshore wind energy is still high compared to other renewable energies (Kost et al., 2013). In order to achieve potential cost reductions of about 30 % in the next ten years (Prognos AG and Fichtner, 2013), a realistic and accurate simulation of offshore wind turbines and their substructures is beneficial. On the one hand, for realistic simulations, the knowledge of scattering environmental conditions is a central point. In this context, scattering conditions are non-constant parameters that exhibit stochastic variations and aleatoric uncertainties, and therefore, should be modelled as statistically distributed. On the other hand, carefully chosen simulation constraints, like the simulation length or the time of initial transients, are essential to obtain accurate results. Here, the simulation length is defined as the usable time for the post-processing. The time of initial transients is the time that is removed from each simulation to exclude initial transients resulting from starting a calculation with a set of initial turbine conditions (like rotor speed). Simulation length plus initial transient time make up the overall length.

Regarding the first point, current guidelines (IEC, 2009) already define that simulations should mirror the changing environmental conditions at the precise site of a wind turbine. However, for academic research, real site data is rarely available, and

even for industrial purposes data quality might be poor for some parameters or long-term data is missing. As a result, various research projects characterised environmental conditions at specific sites or entire areas, and published statistical distributions as a reference. Probably the most frequently used example is the UPWIND design basis (Fischer et al., 2010). Further examples are the work of Stewart et al. (2015), the PSA-OWT project (Hansen et al., 2015), and the investigations by Häfele et al.

5   (2017). All these reference conditions have some limitations. The design basis of Stewart et al. (2015) is only for deep water sites off the coasts of the United States of America. The wave state of deep water sites are not comparable to shallow water conditions in the North Sea, as significant wave heights generally increase with the water depth (Hansen et al., 2015). Additionally, wind speeds are not measured at hub height, and therefore, have to be extrapolated, which increases uncertainties. For the UPWIND design basis, the wind speed is just given at a reference height of 10 m and not at hub height as well. Furthermore,

10   no statistical distributions for conditional parameters (e.g. the wave height H_s depends on the wind speed v_s) are given, but only scatter plots. In the PSA-OWT project, data of the research platform FINO1 in the North Sea is used. Here, the wind speed is measured at hub height, but shadow effects can occur, if sensors are positioned behind the measuring mast. Häfele et al. use data of the research platform FINO3, which has several sensors at each height to reduce shadow effects. However, only five environmental parameters (wind speed and direction, wave height, period and direction) are analysed, and the data period

15   is only five years. Hence, the need for a comprehensive data basis, covering several sites and the most important parameters, becomes obvious in order to enable future research that is based on realistic data. Missing conditions are for example the turbulence intensity, the wind shear or ocean currents.

As to the second point, simulation constraints are frequently chosen based on experience, literature values or recommendations in current standards. However, considering the simulation length and time of initial transients, recommendations in the guide-

20   lines are mainly fairly vague (GL, 2012; IEC, 2009). Simulation lengths of 10 minutes for fatigue calculations (FLS), and one hour or less for ultimate loads (ULS) are frequently recommended. For the initial transients, it is advised to discard 5 seconds or more. Literature values partly differ significantly. To reduce the effects of initial transients, the first 20, 30 or 60 seconds are discarded for example (Vemula et al. (2010); Jonkman and Musial (2010); Hübler et al. (2017)), and simulation lengths of 10 minutes and one hour are common practice (Jonkman and Musial, 2010; Popko et al., 2012; Cheng, 2002). However,

25   longer simulation lengths are partly used as well, especially in the oil and gas industry or for floating substructures (DNV, 2013). Still, all these recommendations are not underpinned with detailed analyses. For floating offshore wind turbines, such investigations were conducted for the simulation length by Stewart et al. (2015), Stewart et al. (2013) and Haid et al. (2013). It is shown that simulation lengths of 10 minutes are sufficient for ULS and FLS loads. The observation that ULS and FLS loads tend to be higher for longer simulations are not due to physical reasons, but to unclosed cycles in the Rainflow counting for

30   the FLS case and a result of the averaging technique in case of ULS loads. Both can be handled by adapting the algorithms. Concerning the time of initial transients, Haid et al. (2013) recommend 60 seconds and the utilisation of initial conditions. This recommendation is based on an analysis which has not been further specified. For a jacket foundation, Zwick and Muskulus (2015) conducted a study investigating lengths of simulations and initial transients and also concluded that 10 minutes are sufficient, as long as 10-minute time series are merged before the Rainflow counting is applied. The required time of initial

35   transients is determined by checking the rotor speed to reach a steady state. However, neither initial conditions are applied,

nor does a steady rotor speed guarantee that all transients are damped out. Therefore, the need for well-founded guidance on simulation lengths and times of initial transients for bottom fixed substructures becomes clear. For the simulation length, useful preliminary work is available, but it is limited to jacket substructures. Concerning initial transients, extensive studies are rare, and do not concentrate on the convergence of the relevant loads (FLS and ULS). Furthermore, scattering environmental

5 conditions are not taken into account. This is a simplification especially in case of the initial transients, as this variation might lead to more pronounced resonance effects (e.g. rarely occurring low wave peak periods that are close to the natural frequency of the structure; cf. Sect. 2.4) and therefore to more pronounced initial transients.

After all, the listed shortcoming in state-of-the-art modelling assistance motivated the current work that focuses on the following aspects:

10 (1) Derive an open access data basis for various scattering environmental conditions at different sites to enable more realistic modelling.

(2) Give well-founded guidance on simulation length requirements and the time needed to exclude initial transients, when these realistic conditions are applied, to improve accuracy of numerical simulations.

In order to address these topics, firstly, a data basis for all significant environmental conditions is derived from real data of the

15 FINO research platforms. In this work, the data source is introduced, the analysis is described, and the resulting distributions and some interesting findings are presented. Secondly, required simulation lengths and times of initial transients are determined. For this purpose, the probabilistic simulation approach and the simulation model are explained. Then, studies of convergence are conducted for the simulation length and the time of initial transients. A monopile and a jacket substructure, FLS and ULS loads, and different wind speeds are considered. Recommendations are summarised. Lastly, the benefits and limitations of the

20 current approach are summarised, and a conclusion is drawn.

2 Comprehensive data basis

2.1 Raw data

Environmental conditions can vary significantly among various turbine sites. As these states affect loads, and therefore, the design of offshore wind turbines, precise data of specific turbine location is valuable. Real site data is scarce, which is the reason

25 for the formerly mentioned reference data bases (Fischer et al., 2010; Hansen et al., 2015; Stewart et al., 2015; Häfele et al., 2017). These data bases define conditional, statistical distributions for some of the most important environmental conditions: Wind speed and direction, wave height, direction and peak period. However, other conditions are fixed for each wind speed or are set completely constant. The states of the frequently used UPWIND design basis are summarised in Table 1 as an example. In this study, scattering conditions are derived directly from offshore measurement data. The raw data is taken from the three

30 FINO platforms, and conditional distributions for the following 13 environmental parameters are determined: wind speed and direction, wave height, peak period and direction, turbulence intensity, wind shear exponent, speed and direction of the sub-

Table 1. Environmental conditions (wind speed v_s, significant wave height H_s, wave peak period T_p, and turbulence intensity TI) of the K13 shallow water site (UPWIND design basis (Fischer et al., 2010)). The wind shear exponent is $\alpha = 0.14$, and wind and wave directions are usually set to zero, but scatter plots are available.

v_s (m s^{-1})	2	4	6	8	10	12	14	16	18	20	22	24	26
TI (%)	29.2	20.4	17.5	16.0	15.2	14.6	14.2	13.9	13.6	13.4	13.3	13.1	13.0
H_s (m)	1.07	1.10	1.18	1.31	1.48	1.70	1.91	2.19	2.47	2.76	3.09	3.42	3.76
T_p (s)	6.03	5.88	5.76	5.67	5.74	5.88	6.07	6.37	6.71	6.99	7.40	7.80	8.14

Figure 1. Positions of the three FINO platforms in the North and Baltic Sea, adapted from OpenStreetMap.

and near-surface current, and air and water density. The FINO measurement masts are located in the North Sea and Baltic Sea, and are operated on behalf of the German Federal Ministry for the Environment, Nature Conservation, Building and Nuclear Safety (BMUB)[1]. The locations of the three FINO sites are marked in Fig. 1.

For all three sites, maximum, minimum, mean, and standard deviation values of the wind speed, measured at different heights between 30 m and 100 m above mean sea level, are available for 10-minute intervals. Wind speeds are measured with cup and ultrasonic anemometers. In this study, cup anemometers are used, as these sensors are available at more different heights. For FINO1 and 2, the anemometers are positioned on jibs in secondary wind directions to reduce shadow effects. For FINO3, three anemometers are installed around the mast to minimise shadow effects. Sensors at different heights allow a detailed analysis of shear effects. Wind direction, air pressure, temperature and humidity are measured at different heights as well. Buoys in the immediate vicinity of the research platforms (about 150 m) measure the wave conditions. Mean values of significant wave heights, wave directions, wave peak periods and water temperatures are measured every 30 minutes. Furthermore, acoustic

---

[1]Raw data of the FINO platforms is freely available for research purposes. See www.fino-offshore.de/en/ for details.

Doppler current profilers (ADCPs) close to the platforms measure ocean current velocities and directions at different water depths using the Doppler effect of sound waves. The platforms FINO1, 2 and 3 have been measuring continuously since 2004, 2007 and 2009 respectively, resulting in 7 to 13 complete years of measurement data, and enabling at least some long-term predictions. Data of incomplete years is not taken into account in order not to introduce bias due to seasonal effects.

2.2 Conditional distributions

In this work, raw data of the FINO measurement masts is used to set up a data base for correlated, scattering environmental conditions. As the post-processing of raw data is time-consuming and unnecessary to be repeated each time environmental conditions are used, conditional probability distributions (i.e. $P(Y = y | X = x)$ with X being the independent random variable, Y the dependent one, and P the probability function) for environmental conditions are derived to make the data base easy to use. Firstly, post-processing is carried out to identify sensor failures (missing data) and measurement failures (outliers). Missing data is not interpolated, but left out, in order not to introduce any bias. As sufficient data of proper signal quality is available (e.g. more than 350 000 data points for the wind speed even for FINO3), this approach is practicable. Wind speed data is synchronised with the wind direction data. This enables a selection of the anemometer in front of the mast for FINO3. For FINO1 and 2, wind speed values are discarded, if the jib is located directly in the tower shadow. The turbulence intensity (TI) can be computed as the quotient of the standard deviation of the wind speed in a 10-minute interval (σ_v) and the mean wind speed in this interval (v_s) according to Eq. (1):

$$\text{TI} = \frac{\sigma_v}{v_s}. \tag{1}$$

For the wind shear, Eq. (2) applies according to the standard IEC 61400-1 (2005):

$$v_s(z) = v_s(z_0) \times \left(\frac{z}{z_0} \right)^{\alpha}, \tag{2}$$

where z is the height above mean sea level, z_0 is a reference height, $v_s(z)$ and $v_s(z_0)$ are wind speeds at the specified heights and α is the wind shear exponent. At the FINO platforms, the wind speed is measured at eight different heights. Therefore, it is possible to determine the wind shear exponent for every 10-minute interval by assuming $z_0 = 90\,\text{m}$ and applying a non-linear regression. The air density can be calculated using Avogadro's Law in Eq. (3) and the measurements of humidity (ϕ), air pressure (p_{humid}), and temperature in degree Celsius (T_{air}):

$$\rho_{\text{air}} = \frac{p_{\text{humid}}}{R_{\text{humid}} T_{\text{air}}}. \tag{3}$$

As humid air can be regarded as a mixture of ideal gases, the following equation applies for R_{humid}:

$$R_{\text{humid}} = \frac{R_{\text{dry}}}{1 - \phi \frac{p_{\text{sat}}}{p_{\text{humid}}} \left(1 - \frac{R_{\text{dry}}}{R_{\text{vapour}}} \right)}, \tag{4}$$

where $R_{\text{dry}} = 287.1 \frac{\text{J}}{\text{kg\,K}}$ is the specific gas constant for dry air, $R_{\text{vapour}} = 461.5 \frac{\text{J}}{\text{kg\,K}}$ for water vapour, and p_{sat} is the saturation vapour pressure that can, for example, be calculated using the August-Roche-Magnus formula:

$$p_{\text{sat}} = 6.1094\,\text{hPa} \times e^{\frac{17.625 \times T_{\text{air}}}{T_{\text{air}} + 243.04}}. \tag{5}$$
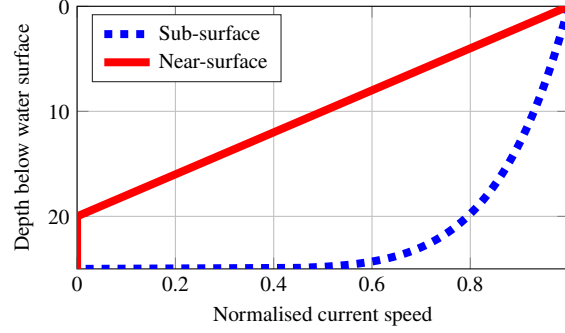
Figure 2. Velocity profiles of the sub- and near-surface currents according to Eqs. (7) and (8) respectively, with a water depth of 25 m and normalised speeds ($v_{\text{SS},0} = v_{\text{NS},0} = 1$)

For the water density, a semi-analytical approach by Millero and Poisson (1981) of the following form is applied:

$$\rho_{\text{water}} = A(T_{\text{water}}) + B(T_{\text{water}})S + C(T_{\text{water}})S^{1.5} + DS^2, \tag{6}$$

where S is the salinity, T_{water} is the water temperature at the surface, A, B and C are polynomial functions of the water temperature and D is a constant. As constant salinity is assumed, the water density is a function of the water temperature. For all wave parameters, three-hour mean values are calculated, as wave conditions stay stationary for a duration of about three hours (GL, 2012). For the speeds and directions of sub- and near-surface currents, measured current values (v_{m} and θ_{m}) have to be converted in order to separate sub- and near-surface components. According to, for example, IEC (2009), the following two equations apply for sub- and near-surface currents respectively:

$$v_{\text{SS}}(z) = v_{\text{SS}}(0\,\text{m})\left(\frac{d-z}{d}\right)^{\frac{1}{7}} \quad \text{and} \tag{7}$$

$$v_{\text{NS}}(z) = \begin{cases} v_{\text{NS}}(0\,\text{m})\left(\frac{20\,\text{m}-z}{20\,\text{m}}\right) & \text{for} \quad z <= 0 \\ 0 & \text{for} \quad z > 0. \end{cases} \tag{8}$$

Here, $v_{\text{SS}}(z)$ and $v_{\text{NS}}(z)$ are the sub- and near-surface current speeds at a position z below the water surface, and d is the water depth. For reasons of clarity, the following notation is introduced: $v_{\text{SS}}(z) = v_{\text{SS},z}$. The velocity profiles are shown in Fig. 2. Obviously, the near-surface current does not exist below a reference depth of 20 m. Hence, it is possible to use measurement data of a depth of 20 m (or more) to directly get the sub-surface direction ($\theta_{\text{SS},20} = \theta_{\text{m},20}$) and to calculate the speed, for example for FINO2 ($d = 25\,m$):

$$v_{\text{SS},0} = v_{\text{SS},20}\left(\frac{25\,\text{m} - 20\,\text{m}}{25\,\text{m}}\right)^{-\frac{1}{7}}. \tag{9}$$

For the near-surface current, measurements close to the surface (e.g. $v_{\text{m},2}$) can be used. However, these measurements include sub- and near-surface components, as shown in Fig. 3. Therefore, the sub-surface component at 2 m has to be calculated
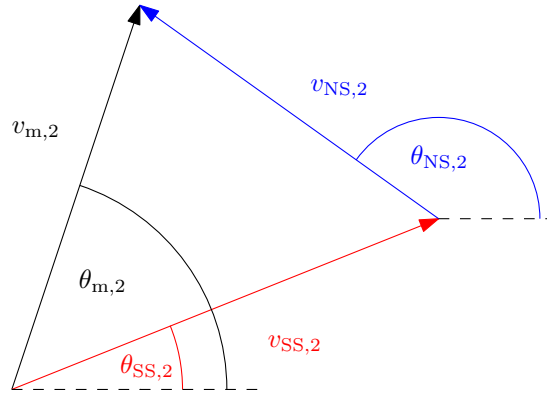
6

Figure 3. Vectorial analysis of ocean current components at a depth of 2 m (measured values (m), near- and sub-surface components (NS and SS))

using Eq. (7), and the sub-surface direction is assumed to be constant over depth ($\theta_{SS,20} = \theta_{SS,2} = \theta_{SS,0}$). Then, trigonometrical relationships can be applied to calculate the near-surface current at 2 m:

$$v_{NS,2} = \sqrt{v_{SS,2}^2 + v_{m,2}^2 - 2v_{SS,2}v_{m,2}\cos(\theta_{m,2} - \theta_{SS,2})} \tag{10}$$

$$\theta_{NS,2} = \theta_{m,2} + \arcsin\left(v_{SS,2}\frac{\sin(\theta_{m,2} - \theta_{SS,2})}{v_{NS,2}}\right) \tag{11}$$

5 Lastly, the reference near-surface current $v_{NS,0}$ is given by:

$$v_{NS,0} = v_{NS,2}\left(\frac{20\,\text{m}}{20\,\text{m} - 2\,\text{m}}\right) \tag{12}$$

A depth-independent near-surface direction is assumed, and therefore, $\theta_{NS,0} = \theta_{NS,2}$.

After having post-processed the measurement raw data, maximum likelihood estimations are applied to the processed data of the regarded 13 environmental conditions in order to fit several statistical distributions. In addition to unimodal distributions,

10 and if several distinct peaks are distinguishable, multimodal distributions are fitted as well, as it is assumed that the peaks are due to physical phenomena. However, as multimodal approaches have more degrees of freedom, they always fit the data better, even in case of a physically unimodal shape. Therefore, they have to be chosen with care in order not to fit physically unimodal distributions with multimodal approaches.

Considering the example of wind speed and wave height, it is self-evident that some environmental parameters are conditioned

15 by others, and dependencies have to be defined. For example, the case of a calm sea during a storm is very unlikely. Analysing scatter plots of the environmental inputs and taking a literature review into account, the dependencies in Table 2 are defined, although it is possible to define them differently (cf. Stewart (2016)), as mainly the correlation is significant, and the determination of cause and effect is secondary.

One of the most common ways to include dependencies in statistical distributions is to split up the data of the depen-

20 dent parameters into several bins of the independent parameters (e.g. Stewart (2016); Johannessen et al. (2002); Li et al.

7

(2015)). To illustrate this approach, for example, the wave peak period is fitted in several bins of 0.5 m wave height (e.g. $P(T_p) = P(T_p|1.5\,\mathrm{m} \leq H_s < 2\,\mathrm{m})$). The bin widths for the dependent parameters are summarised in Table 2 as well. For highly correlated parameters, an alternative to the binning procedure is to model only the deviation between the parameters. Here, the direction of the near-surface current that is highly dependent on the wind direction is an example. Therefore, by modelling the deviation Δ_{NS} according to Table 2, it applies:

$$\theta_{\mathrm{NS}} = \Delta_{\mathrm{NS}} + \theta_{\mathrm{wind}} \tag{13}$$

Visual inspections and objective criteria using Kolmogorov-Smirnov tests (KS tests) and chi-squared tests (χ^2 tests) are used to

Table 2. Dependencies, statistical distributions, and bin widths for environmental conditions derived from FINO1-3 data.

Parameter	Statistical distributions	Dependencies	Bin sizes
Wind speed (v_s)	Weibull	–	–
Wind direction (θ_{wind})	Non-parametric KDE	Wind speed	$2\,\mathrm{m\,s^{-1}}$
Turbulence intensity (TI)	Weibull, gamma	Wind speed	$2\,\mathrm{m\,s^{-1}}$
Wind shear exponent (α_{PL})	Bimodal normal	Wind speed	$2\,\mathrm{m\,s^{-1}}$
Air density (ρ_{air})	Bimodal log-normal	–	–
Significant wave height (H_s)	Gumbel, Weibull	Wind speed	$2\,\mathrm{m\,s^{-1}}$
Wave peak period (T_p)	Bimodal Gumbel	Wave height	$0.5\,\mathrm{m}$
Wave direction (θ_{wave})	Non-parametric KDE	Wave height and wind direction	$1.0\,\mathrm{m}$ and $30°$
Water density (ρ_{water})	Trimodal normal	–	–
Near-surface current (v_{NS})	Weibull	–	–
Sub-surface current (v_{SS})	Weibull, Gumbel	–	–
Deviation NS direction (Δ_{NS})	Bimodal normal	(Wind direction and NS direction)	–
SS direction (θ_{SS})	Non-parametric KDE	–	–

select the best fitting distribution for each environmental condition. Although the KS test is less powerful than other statistical tests, it is still used due to its suitability for small samples (occurring for example for dependent variables and high wind speeds), where χ^2 tests are not applicable. For one parameter, it is attempted to chose only one distribution for all bins and sites in order to keep the data basis easy to use. However, as noted in Table 2, in some cases several distributions are selected to increase the accuracy of the fits.

Directional parameters like θ_{wind} are treated differently, as classical, parametric distributions can hardly fit several peaks in continuous distributions ($0° = 360°$). Therefore, a non-parametric kernel density estimation (KDE) is used to fit directional parameters.
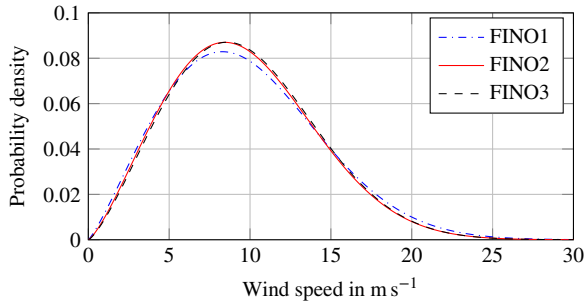
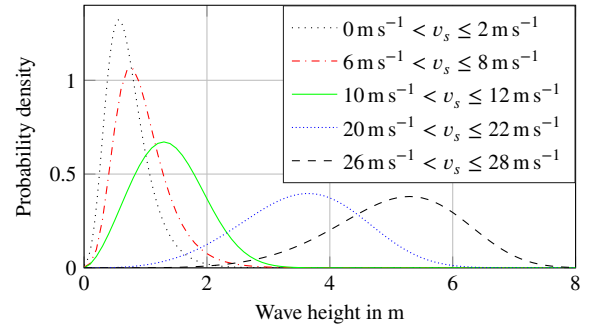**Figure 4.** Weibull distributions for the wind speeds for all three sites

Figure 5. Distribution of the significant wave height for different wind speeds and the FINO1 site. For $v_s \leq 10\,\mathrm{m\,s^{-1}}$, Gumbel distributions are applied. For higher wind speeds, Weibull distributions fit the data more accurately.

2.3 Resulting distributions

In order to establish a full data basis, statistical distribution and their parameters for all thirteen environmental conditions, the three sites and all bins (if necessary) have to be provided. Furthermore, for non-parametric distributions the underlying data is needed. The main ideas are explained here, however, due to the comprehensiveness of the data, detailed and additional information is provided in an easily applicable form, in the supplementary material. At this point, only two examples are shown in Fig. 4 and 5.

2.4 Special findings

In this section, some noteworthy findings of this data basis, mainly resulting from the consideration of scattering, are pointed out. Three examples are presented: the importance of wave peak periods, the high scattering of wind shear exponents, and the behaviour of the turbulence intensity.

Wave loads are of particular importance, if the wave frequency is close to the first natural frequency of the structure. Standard offshore wind turbines have first bending frequencies of about 0.25 to 0.3 Hz (Jonkman and Musial, 2010; Popko et al., 2012) corresponding to eigenperiods of less than 4 s. If state-of-the-art data bases are used (cf. Table 1), there will be no resonance. However, real data suggests that resonance effects are problematic even for higher wind speeds, as wave peak periods of less than 4 s occur (see Fig. 6).

Concerning the wind shear exponent, in the standards and most current data bases (e.g. GL (2012); Fischer et al. (2010)), constant values for all wind speeds are proposed. However, this assumption is a massive simplification. Ernst and Seume (2012) showed that the wind shear exponent significantly depends on the wind speed. Here, it is shown (see Fig. 7) that it does not only vary between wind speeds, but scatters remarkably within each bin as well, and might even be negative.

For the turbulence intensity, this data basis reveals that state-of-the-art approaches are mainly conservative, as too high tur-
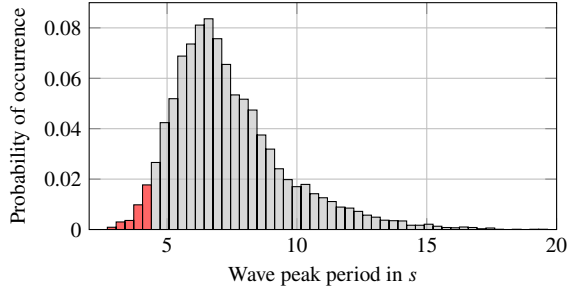
9

Figure 6. Probability distribution of the wave peak period for $v_s = 11\text{-}13\,\mathrm{m\,s^{-1}}$ for the FINO3 site.
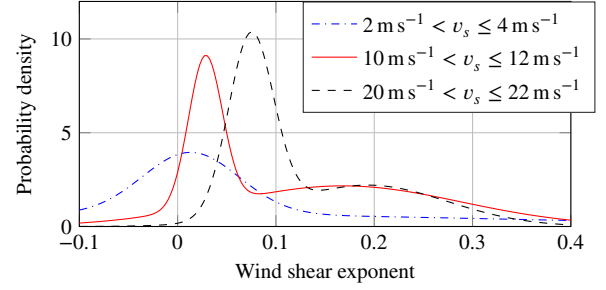

Figure 7. Distribution of the wind shear exponent for different wind speeds for the FINO2 site.
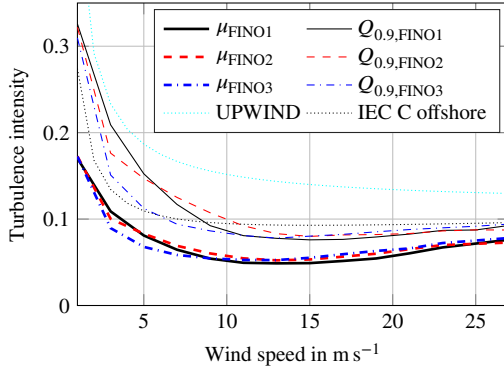

Figure 8. Turbulence intensity (mean value and 90 % percentile ($Q_{0.9}$)) for different wind speeds compared to literature.
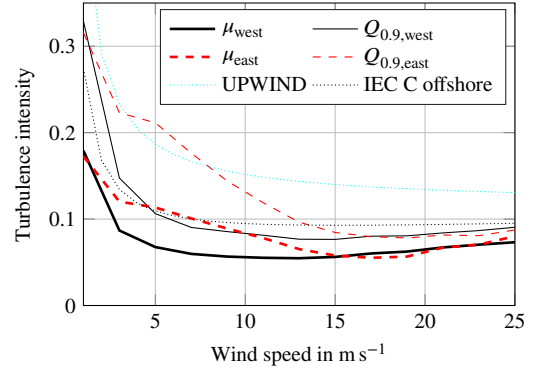

Figure 9. Shadow effects on the turbulence intensity for FINO1 and free stream (western) and wake (eastern) conditions.

bulence intensities are assumed. This is shown in Fig. 8, where the turbulence intensity for all three sites is compared to a standard data basis (Fischer et al., 2010) and to current standards (IEC, 2009). All three sites exhibit similar mean turbulence intensities and 90 % percentile values ($Q_{0.9}$). For the comparison with literature values, the 90 % percentile is of importance, as standards require simulations with this percentile value. However, even for the 90 % percentile, the UPWIND data basis is very

5 conservative. The least conservative case (category C) in IEC (2009) fits the $Q_{0.9}$-values relatively well, but predicts slightly higher turbulence intensities for wind speeds above about $10\,\mathrm{m\,s^{-1}}$. Considering the fact that using the 90 % percentile is a conservative assumption and that the measurements include some wake effects due to wind farms near to all measurement masts, it can be concluded that state-of-the-art assumptions for turbulence intensities are probably unnecessarily conservative. The wake effects are depicted in Fig. 9, where turbulence intensity measurements of FINO1 from 2011 to 2016 are shown. In this period,

10 the wind farm Alpha Ventus was operating on the east side of FINO1. Therefore, west wind leads to free stream conditions and east wind to wake conditions. Obviously, free stream conditions lead to even lower turbulence intensities, whereas wake conditions increase the turbulence especially for smaller wind speeds, as also detected by Hansen et al. (2012).

3 Simulation assistance

In the previous section, a comprehensive data basis for scattering environmental offshore conditions was developed. However, even with realistic input parameters the accuracy of numerical simulations is significantly influenced by constraints like their lengths and the time eliminated to exclude initial transients. Therefore, in this section, efficient simulation lengths and times of initial transients for varying wind speeds and different types of loading and substructures are determined. This is achieved by analysing the convergence of relevant quantities (i.e. FLS and ULS loads). Before conducting these studies, the overall probabilistic simulation approach is explained, as it differs from the approach in the standards. Subsequently, the utilised simulation model and the chosen environmental conditions are briefly presented.

3.1 Probabilistic simulation approach

For the design of offshore wind turbines, several design load cases (DLC1.1 to 8.3) have to be simulated according to the standards (IEC, 2009). These load cases cover ultimate and fatigue loads during power production, idling and fault conditions, and several special cases like start-up or shut-down. Stochastic inputs for turbulent wind and irregular wind are included. Nevertheless, the DLCs remain quasi deterministic, as environmental conditions like turbulence intensities, wind shear, etc. do not scatter. In order to guarantee safe designs despite the deterministic approach, several ULS load cases, covering extreme environmental conditions (e.g. DLC1.3 for turbulence or DLC1.5 for wind shear), are needed.

In this work, statistically scattering environmental conditions are applied, and therefore, a probabilistic simulation approach is used. This probabilistic approach differs from the deterministic load case based approach. For the probabilistic approach or "real-life" approach, it is not necessary to simulate any load cases of extreme environmental conditions (e.g. DLC1.3 to 1.6), but the use of scattering conditions leads directly to simulations that represent the real lifetime of the turbine (without fault, start-up or other special situations). Hence, simulations (e.g. 10000 simulations) cover a realistic period of power production and idling, leading to about 2.3 months of turbine lifetime (for 10000 simulations). As environmental conditions scatter, effects like high turbulences, extreme wind shear, high waves, small wave periods, and others are covered, and do not have to be considered separately. Load cases are not simulated explicitly, but are cover implicitly by conducting probabilistic simulations.

That is why for FLS, the two approaches do not differ significantly. The "real-life" approach covers DLC 1.2 and 6.4. For ULS, the "real-life" approach covers all power production cases (DLC 1.1-1.6) and DLC 6.1 by applying scattering environmental conditions. As the "real-life" approach cannot simulate 20 years of turbine lifetime (or even a return period of 50 years), a load extrapolation, as required for DLC 1.1, is needed in order to calculate an ULS design. However, this extrapolation is not needed here, as it does not influence the investigated simulation constraints.

As common in academia, only power production and idling is simulated. Fault cases, start-up, etc. is not taken into account due to several reasons. Firstly, at least for the jacket, fault cases are less relevant (Vemula et al., 2010). Secondly, these load cases are very controller and design dependent and need special treatment (e.g. there is no need of removing initial transients for start-up load cases). And thirdly, this work is not intended to calculate exact fatigue damages or ultimate loads for the

whole turbine lifetime, as no turbine design or optimisation is done. The exclusion of some load cases does not affect the recommendations on simulations constraints that are given for power production and idling conditions. As there is no need of exact FLS and ULS lifetime loads in this study, an assessment of the probabilistic approach concerning accordance with the standards is neither conducted nor needed, but would be valuable for further applications of probabilistic approaches.

3.2 Simulation setup

As environmental conditions vary for various turbine sites, a data basis being used for the studies of convergence has to be chosen. The basis developed in this work is appropriate, and the FINO3 site is chosen. Some conditions, like air and water density, are kept fixed, as it was shown that their variation is of minor importance (Hübler et al., 2017). It is tried to keep the convergence study as simple as possible, and to focus on the most relevant parameters. Hence, for the probabilistic approach, statistically scattering values according to the determined distributions of wind speed and direction, wave height, direction and period, turbulence intensity, and wind shear exponent are used in all simulations. In addition, the following assumptions are made for all simulations:

- The turbulent wind field is computed according to the Kaimal model and using the software TurbSIM (Jonkman, 2009) with a different wind seed for each simulation.

- Irregular waves are calculated according to the Pierson-Moskowitz spectrum using varying wave seeds for all simulations.

- Soil conditions of the OC3 model (Jonkman and Musial, 2010) are applied.

- The current, second-order and breaking waves, wave spreading effects, marine growth, local vibration effects of braces, joint stiffnesses, and degradation effects are neglected.

The time domain simulations of the convergence study are conducted using the aero-servo-hydro-elastic simulation framework FASTv8 (Jonkman, 2013). A soil model (Häfele et al., 2016) applying linearised soil-structure interaction matrices enhances this code. The NREL 5 MW reference wind turbine (Jonkman et al., 2009) with two different substructures is investigated: Firstly, the OC3 monopile (Jonkman and Musial, 2010) and secondly, the OC4 jacket (Vorpahl et al., 2013). The outcomes of the FAST simulations are, inter alia, time series of forces, moments, and stresses for each element of the substructure.

Since the convergence of fatigue and ultimate loads is investigated in the next step, the calculation concept of these two loads is briefly explained.

For the jacket, the procedure of the fatigue analysis in accordance with DNV-RP-C203 (2010) is the following: For each connection of each joint (K-joints, Y-joint, butt-wlds, etc.), eight hot spot stresses around the circumference of the intersection have to be calculated using the time series. The needed stress concentration factors (SCF) depending on the joint geometry are calculated according Appendix B of DNV-RP-C203 (2010). The fatigue damage is calculated with a fatigue limit of 52.6 MPa at 10^7 cycles. This corresponds to the DNV-GL S-N curve 90 (for cathodic protection) as used in the original design (Vemula et

al., 2010). For all stresses, a Rainflow counting evaluates the stress cycles. As recommended by the current standards, the conservative damage accumulation according to the Palmgren-Miner rule is assumed using a slope of the S-N curve of three before and five after the fatigue limit for both substructures. The separated fatigue calculation (and summation over all simulations) for each connection of each joint is necessary, as damages in each connection and joint are different for each simulation, and

5   the highest values do not always occur in the same joint (for example due to the probabilistic variation of the wind direction). Finally, the decisive damage for the jacket is the highest accumulated value of all connections of all joints.

For the monopile, the fatigue procedure is similar, but is done according to Eurocode 3, part 1-9 (2010), where a detail of 71 MPa for transverse butt welds and an additional reduction due to the size effect ($t > 25$ mm) is recommended. Differing from the recommendations in Eurocode 3, part 1-9 (2010), the same slopes of the S-N-curves as for the jacket are used.

10   For the ULS analysis, maximum stresses are decisive and extracted from the time series. For the monopile, Eurocode 3, part 1-6 (2010), is used to analyse the plastic limit state, cyclic plasticity limit state, and buckling limit state (LS1-3). For the jacket, NORSOK N-004 is applied for tubular members and joints which takes combined axial, shear, bending and hydrostatic loadings into account. In both cases, the yield stress is 355 MPa.

Additionally, ultimate limit state proofs for the foundation piles are performed including axial and lateral soil proofs according

15   to GEO2 (DIN 1054, 2010) and a plastic limit state proof (LS1) for the steel pile below mudline. Especially for the monopile, the last proof might be decisive as the bending moment frequently reaches its maximum below mudline. For all ULS proofs, utilisation factors, being the percentage of the maximum loads, are the outcomes.

3.3   Simulation length

20   The simulation length significantly influences the overall computing time of the load assessment. However, there is no conclusive consensus concerning the length needed. Current standards recommend for example 10-minute or one-hour calculations. The offshore oil and gas industry prefers simulation lengths of six hours to cover all low-frequency hydrodynamic effects.

The use of 10-minute simulations can potentially reduce the computing time by a factor of about 36 compared to six-hour simulations. Hence, a study of convergence for bottom fixed offshore wind turbines is conducted here. For floating wind turbines,

25   it is referred to Stewart (2016), who showed that for floating structures all physical effects can be covered with 10-minute simulations.

The presented outcomes of this study focus on the monopile substructure, but a jacket is analysed as well and results (not shown) are generally comparable. For several wind speed bins, 500 simulations with a total length of ten hours are conducted. As the initial transient behaviour is analysed subsequently, a clearly sufficient time, being discarded to exclude the initial tran-

30   sients, of four hours is chosen. Eliminating these four hours of initial transients, the total length of 10 h reduces to a maximum available length (simulation length) of 6 h for the convergence study. In a first step, the convergence of FLS loads is analysed. Afterwards, the ULS case is investigated.

The procedure to calculate the mean fatigue damage for each wind speed bin is the following: From the basis of the 500 ten-hour simulations having different random seeds and varying environmental conditions, 500 cases are selected (with re-
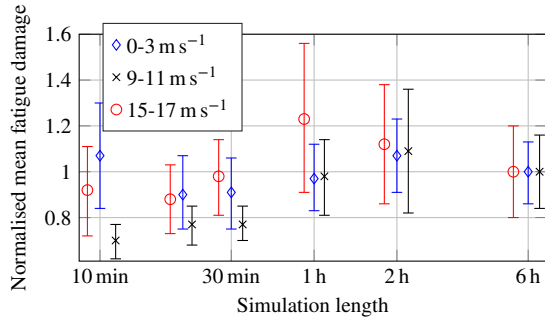
Figure 10. Normalised mean fatigue damage (500 simulations) for increasing simulation lengths and different wind speeds.
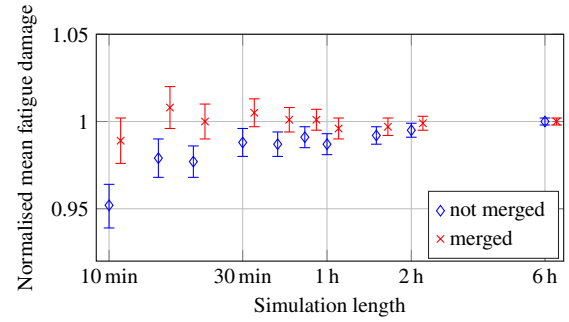
Figure 11. Normalised mean fatigue damage (500 simulations) for increasing simulation lengths and $v_s = 9\text{-}11\,\mathrm{m\,s^{-1}}$. Environmental conditions are kept constant to demonstrate the effect of merging time series more clearly.

placement). For each simulation, the fatigue damage is calculated and weighted with the simulation length. The mean value of all cases is calculated. This procedure is repeated 10 000 times (bootstrapping) to assess the associated uncertainty.

Figure 10 displays the normalised mean fatigue damages for different wind speeds and simulation lengths between ten minutes and six hours. The values are normalised with the six-hour values, and error bars show the $\pm\sigma$ confidence intervals (68 %) that are estimated using a bootstrap procedure with 10 000 resamplings.

It is apparent that due to scattering environmental conditions and the limited number of simulations the uncertainty is relatively high. A detailed investigation of the fatigue load uncertainty, when scattering environmental conditions are applied, is valuable, but out of the scope of this work (cf. Sec. 4). Nevertheless, from Fig. 10 it is apparent that there are no pronounced trends for changing simulation lengths. A slight increase of fatigue loads for higher simulation lengths might be suspected given the fact that such behaviour was observed for floating substructures by Stewart (2016). In order to focus on the simulation length effects, the variation of environmental conditions is neglected in a second step (only varying random seeds). This reduces the uncertainty making it possible to clearly identify a slight increase of FLS loads of about 5 % for higher simulations lengths (see Fig. 11, not merge case). However, as shown by Stewart (2016) for floating substructures, the increasing fatigue loads are not due to any physical effect (all important low-frequency effects of waves are already covered by 10-minute simulations), but can be explained by the effect of unclosed cycles in the Rainflow counting. Cycles that are not completed at the end of the simulation are approximated by counting them as half cycles. The longer the simulation, the less influential is this approximation, as the number of half cycles compared to the number of full cycles reduces. A quite straightforward approach to reduce the problem of half cycles is to merge several shorter simulations (e.g. 10-minute simulations) to a longer one (e.g. six-hour simulation). This means fatigue damages are not calculated for each time series separately, but for longer time series consisting of several shorter ones that are just appended to each other. It is either possible to append different 10-minute time series to each other, or each time series is duplicated and appended several times to itself. If scattering environmental conditions are assumed, in some simulations, fairly different load levels occur. In these cases, load levels of the simulations might not fit,
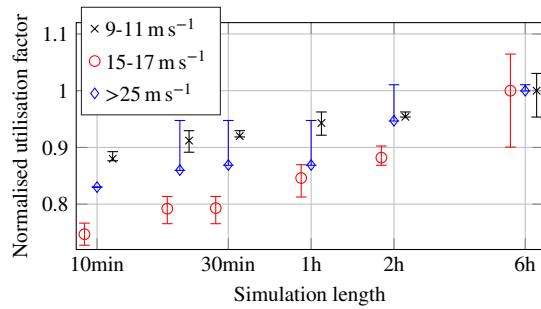
14

Figure 12. Normalised mean ULS utilisation factor (500 simulations) for increasing simulation lengths and different wind speeds.
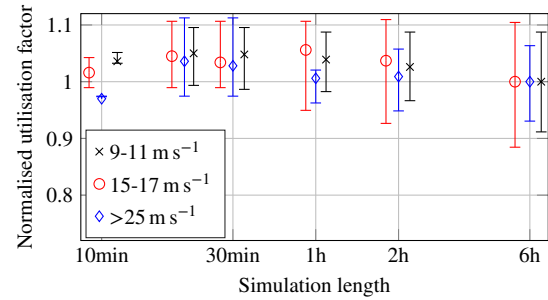
Figure 13. Normalised mean ULS utilisation factor for increasing simulation lengths (constant overall length of 500×10 min leading to 500 to 14 simulations) and different wind speeds.

and additional cycles can be introduced by merging different time series, leading to unreasonably increased fatigue damages. Merging each time series with itself, guarantees fitting load levels. On the downside, the computing time of the post-processing is slightly increased. The effect of merging several shorter simulations with itself to generic and repetitive six-hour time series (e.g. each 10-minute time series is duplicated 36 times and is appended to itself to create a six-hour time series) is demonstrated

5 in Fig. 11. It can be seen that the simulation error of about 5 % too low FLS loads for not merged 10-minute simulations can be compensated by merging time series in the post-processing.

For the ULS loads, the calculation procedure is similar. From the basis of the 500 ten-hour simulations, 500 cases are selected (with replacement). The maximum value of all simulations is taken as decisive utilisation factor. This procedure is repeated 10 000 times (bootstrapping) to assess the associated uncertainty.

10 The convergence is shown in Fig. 12. Obviously, ULS loads are higher for longer simulations. Again, this increase is not due to any physical phenomenon, but a result of different overall computing times. Clearly, 500 10-minute simulations should not be compared to 500 six-hour simulations, but to about 14 six-hour simulations (Haid et al., 2013). Therefore, in a second step, the ULS calculation procedure is slightly adapted. Now, 500 cases are only selected for 10-minute simulations. For all other simulations length, the number of cases is reduced to keep the over simulation length constant at 5 000 minutes (i.e. 250 cases

15 for 20-minute simulation, etc.). This comparison is displayed in Fig. 13 and makes clear that ULS loads do not depend on the simulation length but only on the overall computing time. A second fact being visible in Fig. 13 are the higher uncertainties for longer simulation lengths. Since 10-minute simulations lead to a higher number of cases than six-hour simulations for the same total length (i.e. 500 and 14), shorter simulations better cover rare cases, and therefore, scattering environmental conditions leading to less uncertainty.

20 After all, the investigations of this section suggest that simulations of ten minutes length are sufficient independent of the type of load or investigated substructure, or wind speed. At this point, it has to be noted that only two types of substructures are analysed and environmental conditions typical for the North Sea. For significantly different substructures or locations, the validity might be limited. Notwithstanding the above, for ULS loads, the same overall time has to be compared in order to achieve

15

reliable results. By keeping the simulation length short, more simulations can be conducted in the same overall computing time leading to a better convergence of ULS loads. For FLS loads, simulation errors due to the simulation length can be reduced by merging the time series.

3.4 Initial transients

For the analysis of the simulation length, the first four hours of each simulation were discarded to guarantee a steady state operation of the turbine. However, removing four hours of initial transients and only using ten minutes of simulation is computationally very expensive. Therefore, the convergence of FLS and ULS loads with respect to the time of initial transients is analysed. As initial conditions, like an initial rotor speed, influence the initial transient behaviour (Haid et al., 2013), initial rotor speeds and blade pitches depending on the wind speed are set here. These initial conditions are quasi-static states determined using prior simulations.

As the initial transient behaviour is affected by the type of substructure and the load condition, the time that has to be removed is analysed in each wind speed bin for FLS and ULS loads and for both types of substructures separately. Commonly, time series are investigated to estimate times of initial transients (Zwick and Muskulus, 2015). Although this is a straightforward approach, here, it is considered to be not expedient. For a fatigue assessment, the convergence of the fatigue damage has to be analysed, and for the ULS analysis, maximum loads or utilisation factors have be considered.

For each wind speed bin, 10 000 simulations for the monopile and 500 for the jacket were conducted according to the simulation setup in section 3.2. This means: Each simulation has its own random seed for irregular waves and turbulent wind, and in addition, different wind speeds and directions, wave heights, directions and periods, turbulence intensities and wind shear exponents according to the FINO3 data are applied. The high and unequal number of simulations is needed to exclude effects of the number of simulations, mentioned in the previous section and addressed in Sec. 4, as well as possible. For the monopile, each simulation at operating conditions is 900 s long (600 s simulation length plus 300 s of initial transients) and 1800 s at idling conditions. When the turbine is idling, the aerodynamic damping is lower, leading to more pronounced initial transients. For the jacket, all simulations are 720 s long. Using this simulated data basis, it is possible to analyse the effect of different initial simulation times removed on the fatigue damage and utilisation factors in order to determine optima. The analysed simulation length is kept constant at 600 s while the removed length varies between 0 s and 300 s (1200 s for idling; 120 s for the jacket).

Figure 14 displays the convergence of the fatigue damage of the monopile substructure at operating conditions. Here, 300 s or 120 s values are used as a reference, the so called "converged value". The ten-hour simulations in section 3.3 were used determine these values, where the error due to initial transients can be neglected and is much smaller than the error due to the number of simulations. For idling conditions (not shown), the initial transient behaviour takes longer, as the aerodynamic damping is lower. For the same reason, the transients are shorter for higher wind speeds. For the jacket substructure displayed in Fig. 15, the transients decay much faster in all wind speed bins. As jackets are less influenced by wave loads, being not always aligned with the wind, the aerodynamically marginally damped side-to-side modes are less excited, leading to a shorter transient behaviour. This interpretation is supported by the fact that for the jacket, idling conditions, where the hydrodynamic
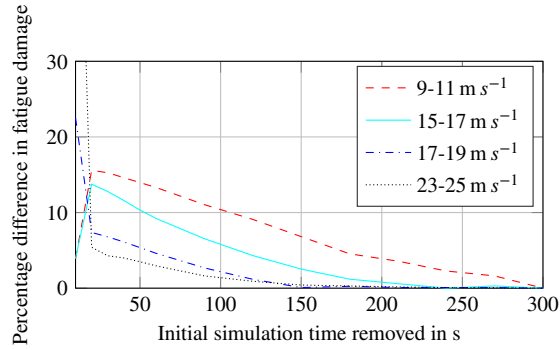
16

Figure 14. Initial transient behaviour of the operating wind turbine with a monopile substructure for different wind speeds. Percentage difference in the fatigue damage compared to the "converged" value (300 s).
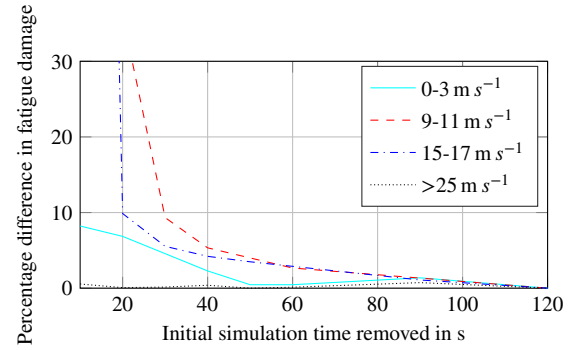
Figure 15. Initial transient behaviour of the wind turbine with a jacket substructure for different wind speeds. Percentage difference in the fatigue damage compared to the "converged" value (120 s).

behaviour dominates, have shorter initial transients.

The convergence of ULS utilisation factors for both substructures is shown in Fig. 16 and 17. It becomes apparent that initial transients are short independent of the type of substructure and wind speed. The cycles with high amplitudes occurring at the beginning of each simulation are damped out within a few seconds, and hence, are not influencing the ULS behaviour. More problematic are less damped cycles with smaller amplitudes leading to the previously presented, higher times of initial transients for FLS loads.

The recommended times that should be discarded to exclude initial transients for both substructures, being always a compromise between computing time and accuracy (here, errors below 5 %), are summarised in Table 3. It has to be mentioned that the general validity is limited, as these times of initial transient might vary for example for different aero-elastic codes, numerical solvers, time constants of the aero-elastic models, or substantially different substructures. For example, jackets for 10 MW turbines might behave differently due to larger diameters of legs and braces increasing wave effects. However, for similar applications (e.g. FASTv8, NREL 5 MW turbine, OC3 monopile or OC4 jacket, etc.) that are not rare in academia (e.g. Zwick and Muskulus (2015) or Morató et al. (2017)), the given values represent a well-founded guidance for simulation set-ups. Furthermore, these results shall sensitise the research community to the problem of initial transients especially in case of fatigue. For fatigue, the time of initial transients might be higher than frequently presumed in literature. This is due to weakly damped cycles with small amplitudes that cannot directly be identified when looking at time series.

4   Benefits and limitations

The benefit of the current work is twofold. Firstly, a comprehensive data basis for scattering environmental conditions was set up, which is freely available and easy to use. Secondly, two simulation constraints (simulation length and time of initial
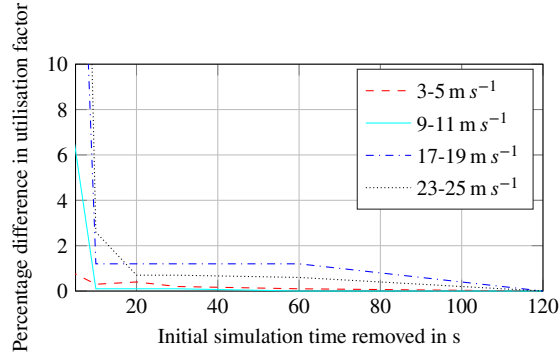
17

Figure 16. Initial transient behaviour of the wind turbine with a monopile substructure for different wind speeds. Percentage difference in the utilisation factor (ULS) compared to the "converged" value (120 s).
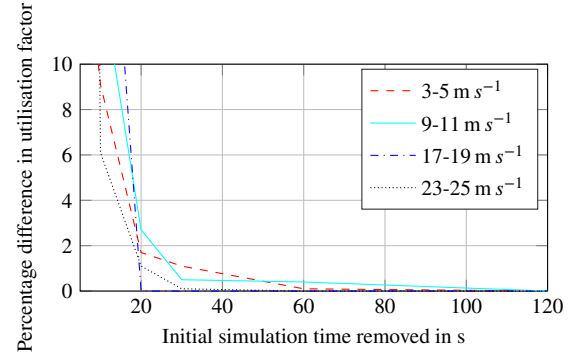

Figure 17. Initial transient behaviour of the wind turbine with a jacket substructure for different wind speeds. Percentage difference in the utilisation factor (ULS) compared to the "converged" value (120 s).

Table 3. Recommended times that should be discarded to exclude initial transients for simulations with OC4 jacket and OC3 monopile substructures for different wind speeds to achieve errors below 5 %.

v_s in m s^{-1}	Case	< 3	3-5	5-7	7-9	9-11	11-13	13-15	15-17	17-19	19-21	21-23	23-25	> 25
Monopile	FLS	720 s	240 s	240 s	240 s	240 s	240 s	240 s	150 s	120 s	60 s	60 s	60 s	360 s
Jacket		40 s	30 s	50 s	40 s	50 s	50 s	50 s	50 s	50 s	60 s	50 s	50 s	10 s
Monopile	ULS	<10 s	<10 s	<10 s	<10 s	10 s	10 s	10 s	10 s	10 s	10 s	10 s	10 s	<10 s
Jacket		<10 s	20 s	20 s	20 s	20 s	20 s	20 s	20 s	20 s	20 s	20 s	20 s	<10 s

transients) were analysed, and well-founded recommendations are given.

The main advantages over existing data bases are the following: The data basis covers several different sites being situated in different oceans. It has to be admitted that the sites are fairly similar, as they are all in shallow water conditions. Additionally, the data basis contains statistical distribution for much more environmental conditions than existing ones. As was shown for example by Hübler et al. (2017) that not only main conditions like the wind speed are influencing the dynamic behaviour of offshore wind turbines, knowledge of additional parameters is beneficial. Current data bases consist frequently of raw data that needs to be post-processed, which is a time-consuming process. Here, on the one hand, easily applicable statistical distributions are given. One the other hand, the complexity of dependent environmental conditions is still covered by utilising conditional distributions and multimodal and non-parametric approaches. In contrast to many existing data bases, the raw data is of good quality. For example, wind speeds are measured at heights comparable to hub heights of current turbines, and there is no need for extrapolations, as it is the case for buoy measurements. Still, more data would be valuable in order to achieve more reliable distributions in high wind speed bins that rarely occur. After all, the developed data basis is capable to improve offshore wind

18

turbine modelling by providing more realistic inputs for simulations in academia where real site data is scarce. One example of improved offshore wind turbine modelling is given in Sec. 3.3 and 3.4. The inclusion of probabilistic inputs leads to a significant and realistic increase of fatigue damage scattering requiring high numbers of simulations. Hence, deterministic inputs underestimating this scattering can lead to biased fatigue values. Detailed analyses of the effect of scattering environmental conditions on fatigue damage, and therefore, of the needed number of simulations are part of upcoming work of the authors. Concerning the second benefit, the simulation constraints, it has to be kept in mind that not only realistic modelling, but also small simulation errors are important in order to model accurately. In this context, the chosen simulation length and time of initial simulation transients matter. So far, these values are frequently chosen without profound knowledge. Some approaches to gain a deeper insight into these constraints (Stewart, 2016; Zwick and Muskulus, 2015) concentrate on simulation lengths or specific types of substructures and are not taking realistically scattering environmental conditions into account. In this work, the scattering of the conditions is addressed and different bottom fixed substructures are analysed. This enables recommendations for simulation lengths and times of initial transients depending on the wind speed, the type of substructure and the considered load case (ULS or FLS). However, the general validity of the current results has to be slightly restricted, as only one design of each type of substructure was investigated. Therefore, the initial transient behaviour might be slightly different for significantly different designs. Furthermore, for the time being removed to exclude initial transients, the values might also differ between different simulation codes and are only tested for the FASTv8 code. Different numerical solver or time constants of the aero-elastic models might also influence the time of initial transients. Nevertheless, even in these cases, the given recommendations can be regarded as a well-founded starting point for further investigations, and, even more important, clarify the challenge of a well-founded choice.

5 Conclusions

This work aims to help future simulation work to be more realistic and accurate. In order to achieve this objective, a freely available and comprehensive data basis for scattering environmental conditions was set up. This data basis consists of conditional statistical distribution for many parameters and can be applied without further post-processing. All needed information (statistical distribution and their parameters) is given in the supplementary material. In academia, this data basis enables simulations with probabilistic environmental conditions making them more realistic. For industry purposes, this work might lead to a reconsideration of the current practice. This study shows that the use of deterministic values being either only dependent on the wind speed (e.g. turbulence intensity) or even totally constant (e.g. wind shear) does not represent realistic offshore conditions. However, for a well-founded reconsideration of the current practice, a detailed assessment of probabilistic approaches compared to deterministic load case based ones is needed.

Additionally, scientifically sound recommendations are given for the choice of simulation lengths and times to be removed to exclude initial transients. Simulation lengths of 10 minutes are generally sufficient, and can even help to reduce uncertainties. However, in case of FLS loads, times series should be merged, and for ULS situations, the overall computing time has to be kept constant. Recommendations concerning the initial transients have to be handled with care due to limitations of the general

19

validity. The values are summarised in Table 3 and can help to improve the accuracy of simulations, and to reduce computing times. It should be noted that a partly significantly longer initial transient behaviour compared to values in literature, being mainly based on educated guesses, was detected.

An enlargement of the current data basis to include additional offshore sites, other types or designs of substructures or investigations for other simulation codes and numerical solver would be definitely valuable to increase the general validity. Furthermore, even for the utilised FAST code, additional investigations concerning the amount of eigenmodes representing the substructure would be beneficial, as a reduction of retained eigenmodes might reduce the time of initial transients.

References

Cheng. P. W.: A reliability based design methodology for extreme responses of offshore wind turbines, DUWIND Delft University Wind Energy Research Institute, 2002.

Det Norske Veritas: Fatigue design of offshore steel structures, Recommended practice DNV-RP-C203, 2010.

5 Det Norske Veritas: Design of floating wind turbine structures, Offshore Standard DNV-OS-J103, 2013.

DIN - Normenausschuss Bauwesen: Subsoil - Verification of the safety of earthworks and foundations - Supplementary rules to DIN EN 1997-1, DIN 1054, 2010.

Ernst, B. and Seume, J. R.: Investigation of site-specific wind field parameters and their effect on loads of offshore wind turbines, Energies, 5, 3835-3855, 2012.

10 European Committee for Standardization: Eurocode 3: Design of steel structures - Part 1-6: Strength and stability of shell structures, EN 1993-1-6, 2010.

European Committee for Standardization: Eurocode 3: Design of steel structures - Part 1-9: Fatigue, EN 1993-1-9, 2010.

Fischer, T., de Vries, W., and Schmidt, B.: Upwind Design Basis, 2010.

Germanischer Lloyd: Guideline for the Certification of Offshore Wind Turbines, Offshore Standard, 2012.

15 Häfele, J., Hübler, C., Gebhardt, C. G., and Rolfes, R.: An improved two-step soil-structure interaction modeling method for dynamical analyses of offshore wind turbines, Applied Ocean Research, 55, 141-150, 2016.

Häfele, J., Hübler, C., Gebhardt, C. G., and Rolfes, R.: Effcient Fatigue Limit State Design Load Sets for Jacket Substructures Considering Probability Distributions of Environmental States, The 27th International Ocean and Polar Engineering Conference, 2017.

Haid, L., Stewart, G., Jonkman, J., Robertson, A., Lackner, M., and Matha, D.: Simulation-length requirements in the loads analysis of
20 offshore floating wind turbines, 32nd International Conference on Ocean, Offshore and Arctic Engineering, ASME, 2013.

Hansen, K. S., Barthelmie, R. J., Jensen, L. E., and Sommer, A.: The impact of turbulence intensity and atmospheric stability on power deficits due to wind turbine wakes at Horns Rev wind farm, Wind Energy, 15, 1, 183-196, 2012.

Hansen, M., Schmidt, B., Ernst, B., Seume, J., Wilms, M., Hildebrandt, A., Schlurmann, T., Achmus, M., Schmoor, K., Schaumann, P., Kelma, S., Goretzka, J., Rolfes, R., Lohaus, L., Werner, M., Poll, G., Böttcher, R., Wehner, M., Fuchs, F., and Brenner, S.: Probabilistic
25 Safety Assessment of Offshore Wind Turbines, Leibniz Universität Hannover, 2015.

Hübler, C., Gebhardt, C. G., and Rolfes, R.: Hierarchical Four-Step Global Sensitivity Analysis of Offshore Wind Turbines Based on Aeroelastic Time-Domain Simulations, Renewable Energy in press.

International Electrotechnical Commission: Wind turbines - part 1: Design requirements, International standard IEC 61400-1, 2005.

International Electrotechnical Commission: Wind turbines - part 3: Design requirements for offshore wind turbines, International standard
30 IEC 61400-3, 2009.

Johannessen, K., Meling, T. S., and Hayer, S.: Joint distribution for wind and waves in the northern north sea, International Journal of Offshore and Polar Engineering, 12, 1, 1-8 2002.

Jonkman, B. J.: TurbSim user's guide: Version 1.50, National Renewable Energy Laboratory, 2009.

Jonkman, J.: The New Modularization Framework for the FAST Wind Turbine CAE Tool, 51st AIAA Aerospace Sciences Meeting, including
35 the New Horizons Forum and Aerospace Exposition, 2013.

Jonkman, J., Butterfield, S., Musial, W., and Scott, G.: Definition of a 5 MW Reference Wind Turbine for Offshore System Development, National Renewable Energy Laboratory, 2009.

Jonkman, J. M. and Musial, W.: Offshore Code Comparison Collaboration (OC3) for IEA Task 23 Offshore Wind Technology and Deployment, National Renewable Energy Laboratory, 2010.

Kost, C., Mayer, J. N., Thomson, J., Hartmann, N., Senkpiel, C., Philipps, S., Nold, S., Lude, S., and Schlegl, T.: Stromgestehungskosten erneuerbare Energien. Fraunhofer-Institut für solare Energiesysteme ISE, 2013.

5 Li, L., Gao, Z., and Moan, T.: Joint distribution of environmental condition at five european offshore sites for design of combined wind and wave energy devices, Journal of Offshore Mechanics and Arctic Engineering, 137, 031901, 2015.

Millero, F. J. and Poisson, A.: International one-atmosphere equation of state of seawater, Deep Sea Research Part A. Oceanographic Research Papers, 28, 6, 625-629, 1981.

Morató, A., Sriramula, S., Krishnan, N., and Nichols, J.: Ultimate loads and response analysis of a monopile supported offshore wind turbine

10 using fully coupled simulation, Renewable Energy, 101, 126-143, 2017.

Moriarty, P. J., Holley, W. E., and Butterfield, C. P.: Extrapolation of extreme and fatigue loads using probabilistic methods, National Renewable Energy Laboratory, 2004.

Popko, W., et al. Offshore Code Comparison Collaboration Continuation (OC4), Phase 1-Results of Coupled Simulations of an Offshore Wind Turbine With Jacket Support Structure, The Twenty-second International Offshore and Polar Engineering Conference. International

15 Society of Offshore and Polar Engineers, 2012.

Prognos AG and Fichtner: Kostensenkungspotenziale der Offshore-Windenergie in Deutschland, Stiftung Offshore-Windenergie, 2013.

Stewart, G. M.: Design Load Analysis of Two Floating Offshore Wind Turbine Concepts, PhD-thesis, University of Massachusetts, 2016.

Stewart, G., Lackner, M., Haid, L., Matha, D., Jonkman, J., and Robertson, A.: Assessing fatigue and ultimate load uncertainty in floating offshore wind turbines due to varying simulation length, Safety, Reliability, Risk and Life-Cycle Performance of Structures and Infras-

20 tructures, 239-246, 2013.

Stewart, G. M., Robertson, A., Jonkman, J., and Lackner, M. A.: The creation of a comprehensive metocean data set for offshore wind turbine simulations, Wind Energy, 19, 1151-1159, 2015.

Vemula, N. K., de Vries, W., Fischer, T., Cordle, A., and Schmidt, B.: Design Solution for the UpWind Reference Offshore Support Structure - Deliverable D4.2.5 (WP4: Offshore Foundations and Support Structures), Rambøll Wind Energy, 2010.

25 Vorpahl, F., Popko, W., and Kaufer, D.: Description of a basic model of the 'UpWind reference jacket' for code comparison in the OC4 project under IEA Wind Annex 30, Fraunhofer IWES, 2013.

Zwick, D. and Muskulus, M.: The simulation error caused by input loading variability in offshore wind turbine structural analysis, Wind Energy, 18, 1421-1432, 2015.